IEEE Access
Multidisciplinary | Rapid Review | Open Access Journal

Received June 15, 2016, accepted July 12, 2016, date of publication July 14, 2016, date of current version August 4, 2016.

Digital Object Identifier 10.1109/ACCESS.2016.2591535

Piezoelectric vs. Capacitive Based Force Sensing in Capacitive Touch Panels

SHUO GAO, VICTOR ARCOS, AND AROKIA NATHAN, (Fellow, IEEE)
University of Cambridge, Cambridge CB2 1TN, U.K.
Corresponding author: S. Gao (sg690@cam.ac.uk)

ABSTRACT High sensitivity force sensing is a desirable function of capacitance touch screen panels. In this paper, we report on a dynamic force detection technique by utilizing piezoelectric materials. The force-voltage responsivities are investigated for four widely used stack-ups, with various panel thicknesses and touch locations. Based on the theoretical analysis and simulation results, the maximum responsivity and the signal-to-noise ratio are achieved at 0.42 V/N and 59.1 dB, respectively. The proposed technique implements force sensing successfully, enhancing the human–machine interactivity experience.

INDEX TERMS Force sensing, capacitive touchscreen panel, sensitivity, piezoelectric film.

I. INTRODUCTION

Capacitance touch screen panels (TSP) are widely used in displays, as they offer benefits such as multi-touch, high visibility, and non-physical touch recognition[1]. Traditional capacitance TSPs provide 2D (x-y coordinate) touch detection [2], while 3D (z coordinate indicates force level) touch detection has been achieved recently [3].

In [3], the displacement of the touch location is utilized to represent the force level. Capacitive sensors are integrated into the backlight of the display for measuring the distance change between the cover glass and the backlight. However, when a force touch happens near the edge of the touch panel, the small displacement challenges the detection accuracy. In [3] only two force sensing levels are supported, which cannot provide good user experience especially for drawing applications.

This paper will outline a new strategy that aims to tackle this very problem. It is an approach to implement force sensing in capacitance TSPs by employing piezoelectric materials [4], [5] which generate charges on the surface when a force load is applied. The amount of charge produced is proportional to the strength of the force and the piezoelectric film thickness. Thus when the piezoelectric material is used as substrate of the touch sensors, the induced charge can be read by the touch sensors for force sensing.

Four stack ups widely used in industry are investigated, and one of them is depicted in Fig. 1. A thin layer of the piezoelectric film ($\sim 10\mu$m) is underneath the touchscreen glass ($\sim$0.5mm). The electrodes are much thinner compared to the piezoelectric film and cover glass so they are not shown in the figure. When a force is applied to the glass surface, the stress transmitted to the piezoelectric film layer will result in the induction of charges, which will be measured to interpret the force level. Among the four stack-ups, the highest responsivity and signal-to-noise ratio (SNR) are 0.42 V/N and 59.1 dB respectively, indicating that the applied force can be accurately interpreted.

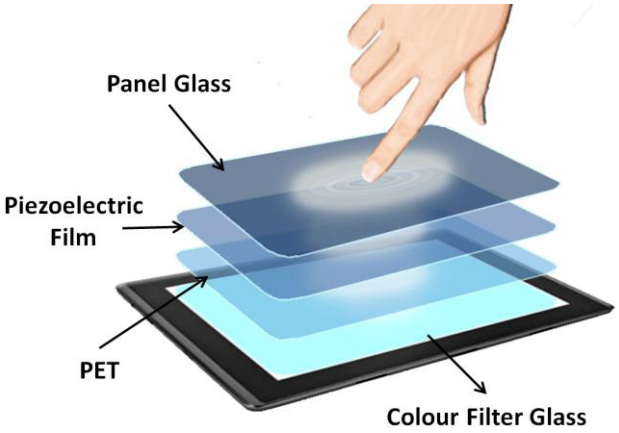

FIGURE 1. One stack-up of the piezoelectric film based capacitive touch screen panel.

This paper is structured as follows. Section II covers a review of piezoelectric mechanism. In Section III, the force sensing technique is presented and four stack-ups are proposed and the corresponding mechanical analyses are given in Section IV. The simulation results and related analyses are provided in Section V, followed by conclusions.

II. PIEZOELECTRIC FORCE SENSING

Piezoelectricity is the phenomenon by which charges are generated by some solid materials when mechanical stress is applied [6]. It was first demonstrated in 1880 by C. Linnaeus and F. Aepinus. The working principle of the piezoelectric materials is based on their non-Centrosymmetric structures. When a load force is applied to a Centrosymmetric material, its polarization remains intact. In contrast, the polarization of non-Centrosymmetric material moves positive or negative in according to the direction of the applied force. A variety of piezoelectric materials are available, such as polyvinylidene difluoride (PVDF) [4], quartz [7] and Piezopaint [8]. In the following paragraph, the relationship between applied force, generated charge and corresponding voltage is explained.

The induced polarization of a piezoelectric film and the stress tensor have a linear relationship [9],

$$P_i = d_{ijk}\sigma_{jk} \quad \text{with } i, j, k = 1, 2, 3 \tag{1}$$

where P_i is the induced polarization, σ_{jk} and d_{ijk} denote the stress and piezoelectric coefficient respectively. The coefficients remain the same for direct and inverse piezoelectric effects. The coefficients d_{ijk} are symmetric in j and k [10]. Thus Eq. 1 can be simplified as

$$P_i = d_{ij}\sigma_j \quad \text{with } i = 1, 2, 3 \quad \text{and } j = 1, 2, \ldots, 6 \tag{2}$$

If 1 N/m^2 mechanical stress is applied perpendicularly to the surface of the piezoelectric film, then the coefficient d is determined by the density of the charge that is accumulated on its surface. The induced polarization P leads to surface charge (Q), this is expressed as

$$Q = AP; \tag{3}$$

where A is the contact area. The induced voltage is expressed as

$$V = Q/C = tP/\varepsilon_0\varepsilon_r \tag{4}$$

where t is the thickness of piezoelectric film, $\boldsymbol{\varepsilon}_0$ is vacuum permittivity and $\boldsymbol{\varepsilon}_r$ is the relative permittivity of piezoelectric material. By measuring the induced voltage, we can calculate the stress and further learn the applied force. Piezoelectric materials are widely used in a variety of applications [15]–[25].

III. METHOD DESCRIPTION

PROPOSED STACK-UPS

The top view and cross-section views of the four proposed stack-ups are depicted in Fig. 2. Their mechanical properties for different piezoelectric film thicknesses are investigated. The parameters of the materials are illustrated in Table 1. Electrode layers are not depicted as they are very thin compared to the other layers. Electrodes will not affect the mechanical investigation. To investigate the mechanical response of the proposed stack-ups, 13 touch locations evenly distributed throughout the touch panel are investigated. Due to the symmetric property of the touch locations, only 5 of them are analyzed, as depicted in Fig. 2 (e).

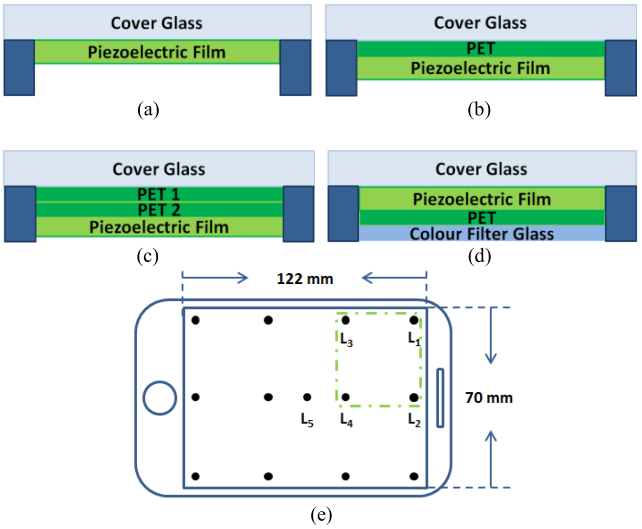

FIGURE 2. Four proposed stack-ups of touch panels (a) – (d), the electrodes are on and underneath the piezoelectric film layer. Top view of proposed touch panel and investigated touch locations (e).

TABLE 1. Parameters of the proposed stack-ups.

	Thickness (m)	Length (mm)	Width (mm)
Panel Glass	0.5×10^{-3}	122	70
Piezo. Film	(10, 25, 50 100) $\times10^{-6}$	122	70
PET	50×10^{-6}	122	70
Colour Filter Glass	0.4×10^{-3}	122	70

TABLE 2. Mechanical and piezoelectrical properties of stack-ups.

	Young's Modulus (Pa)	Poisson Ratio	Density (kg/m^3)	Piezo. Coeff. (nC/N)
Panel Glass [11]	7.4×10^{10}	0.3	2200	———
Piezo. Film [12]	8.3×10^{9}	0.18	1780	38
PET [13]	3.1×10^{9}	0.37	1380	———
Colour Filter Glass[14]	7.5×10^{9}	0.25	2500	———

IV. MECHANICAL ANALYSIS OF PROPOSED TOUCH PANELS

In this section, we analyze the mechanical response of the touch panel to force touches. Here, the relationship between force, stress, strain, panel thickness and displacement is investigated.

The force is assumed to be uniformly distributed over the contact area. The boundary conditions of the touch panel lie between a simple supported case and a fully clamped case. For the latter, there is little literature available due to its high complexity. Thus, numerical results from finite element simulation software (COMSOL) are used for analysis. In this section, only the simply supported case is investigated.

Furthermore, as the thickness and Young's modulus of the glass panel are much bigger than those of other layers Table 2, the glass panel dominates in the mechanical analysis. As a result the other layers are neglected.

Navier-Stokes double Fourier series solution [21] is used to obtain the displacement at a particular position (x, y) from a point force applied at a particular location (ζ, η). Some of the assumptions of Kirchhoff-Love plate theory are as follows:

1. The thickness of the plate is much smaller than all the other physical dimensions
2. The displacements of the plate are small compared to the plate thickness
3. The material is linear elastic
4. Plane strains are small compared to unity

Our model meets all of these criteria. The closed-form solution is expressed as:

$$w(x, y, \xi, \eta) = \frac{\sum_{n=1}^{\infty}\sum_{m=1}^{\infty} \frac{4}{\pi^4 abD} \sin(\frac{n\pi x}{a}) \sin(\frac{m\pi y}{b}) \sin(\frac{n\pi \xi}{a}) \sin(\frac{m\pi \eta}{b})}{(\frac{n^2}{a^2} + \frac{m^2}{b^2})^2}$$

where

$$D = \frac{Et^3}{12(1-\nu^2)}; \tag{5}$$

The stress in the z direction is assumed to be 0 since the material is very small in the z direction compared to the other dimensions. Therefore only plane stresses are considered. The stresses and in the x and y directions and the shear stress in the x-y plane can be found from the following expression:

$$\begin{pmatrix} \sigma_{xx} \\ \sigma_{yy} \\ \tau_{xy} \end{pmatrix} = \frac{-Ez}{1-n^2} \begin{bmatrix} 1 & \nu & 0 \\ \nu & 1 & 0 \\ 0 & 0 & \frac{1+\nu}{2} \end{bmatrix} \begin{bmatrix} \frac{\partial^2 \omega}{\partial x^2} \\ \frac{\partial^2 \omega}{\partial y^2} \\ 2\frac{\partial^2 \omega}{\partial x \partial y} \end{bmatrix}; \tag{6}$$

Based on the above equations, the closed-form relationship between force, stress and displacement is depicted in Fig. 3. Numerical results from COMSOL are shown together with closed-form solution in Fig. 3. The good alignment validates the accuracy of COMSOL as a simulator.

V. RESULTS AND DISCUSSION

In the previous section, the theoretical analysis of a simply supported plate was investigated. Due to the lack of literature on the fully clamped case, in this section, simulation results from COMSOL are utilized to analyze the resolution and sensitivity for displacements of the touch panel and stresses on the piezoelectric film. The results for location 1 and 5 of stack-up 1 are illustrated, as stack-up 1 has the lowest panel thickness and consequently the largest displacement among the four stack-ups. Locations 1 and 5 represent two extreme cases. Uniform forces over small concentric circles of radius 1mm are applied at locations 1 to 5, with different strength levels (0.1N to 1N).

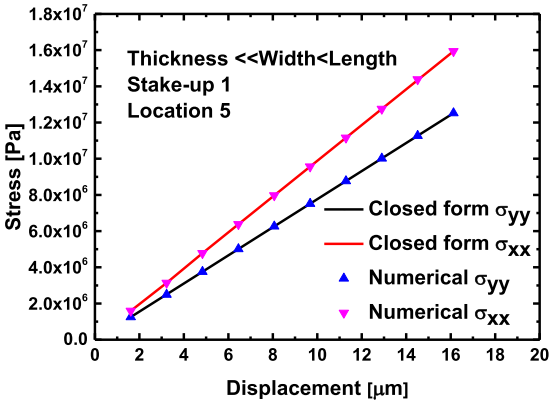

FIGURE 3. Force vs. Stress and Force vs. Displacement when thickness is 0.5mm at location 5.

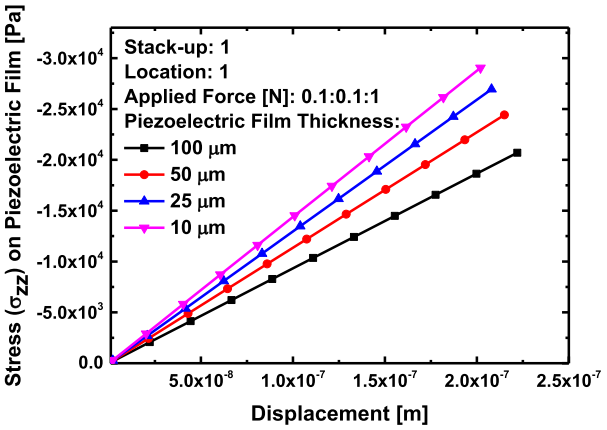

(a)

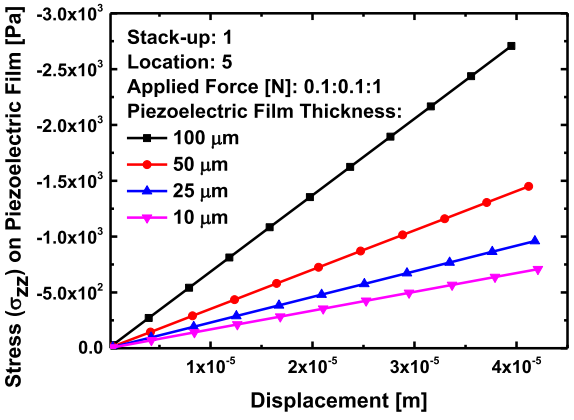

(b)

FIGURE 4. Resolution results for stackup 1: (a) displacement and (b) stress.

The simulation results are depicted in Fig. 4. As described previously, five touch locations were investigated, which can be divided into two scenarios. Locations 4 and 5 are at and near the center region of the panel, thus can be explained by fully clamped plate theory. In contrast, locations 1 to 3 are close to the edges of the plate, hence they are approximated in a better way by axial compression in the z plane.

From Fig. 4, it can be observed that with the increment of piezoelectric film thickness, the displacements and stresses at locations 4 and 5 drop, which aligns with our expectation. However, at locations 1 to 3, the displacements increase, together with the piezoelectric film thickness. This is because when the edges of the plate are fixed, the displacement is purely due to the compressive strain in the z direction. As the thickness goes up the strain will therefore increase, since the piezoelectric film has a lower Young's modulus than the glass. This also explains the stress resolution results.

As the frames support the whole panel, most of the stress is concentrated at the frame regions. That is the reason why the stress values of location 4 and 5 are much smaller than those at locations 1 to 3, while location 1 has the highest stress value.

To further examine the proposed technique, we laminate a layer of piezoelectric film ($d_{33} = 20$pC/N) with a commercial touch panel (Microchip Inc). When a 1N perpendicular touch happens at the center of the panel edge, the output signal peaks at 0.2V (as shown in Fig. 5), indicating high force sensitivity.

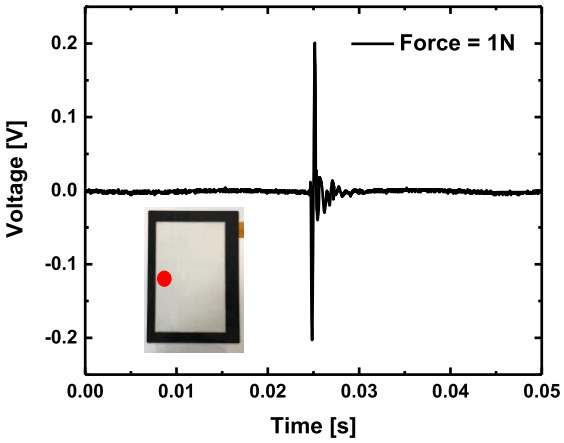

FIGURE 5. Voltage response of a 1N perpendicular force at the center edge of the piezo film laminated touch panel. The red point indicates the touch location. The actural contact area is 1mm^2.

From the simulation and experimental results, a good responsivity can be achieved at 0.42 V/N. However, noise could affect signal detection, especially the system's sensitivity. Therefore a SNR analysis has been carried out.

A. SNR ANALYSIS

The force applied to the touch panel needs to be converted into an electric signal for the processor to manipulate. Henceforth, a transimpedance amplifier (TIA) is employed as the readout circuit. The SNR is an important parameter for a sensing system. In this section we theoretically analyze the SNR value for the presented piezoelectric film based force sensing system.

Piezoelectric films can be modeled as a charge generator in parallel with a capacitor (C_{PF}) and an internal film resistor (R_{PF}) [28] as depicted in Fig. 6 (a). Due to the fact that different circuit designs contribute to various noise components, a typical charge amplifier is analyzed as an example. This is shown in Fig. 6 (b).

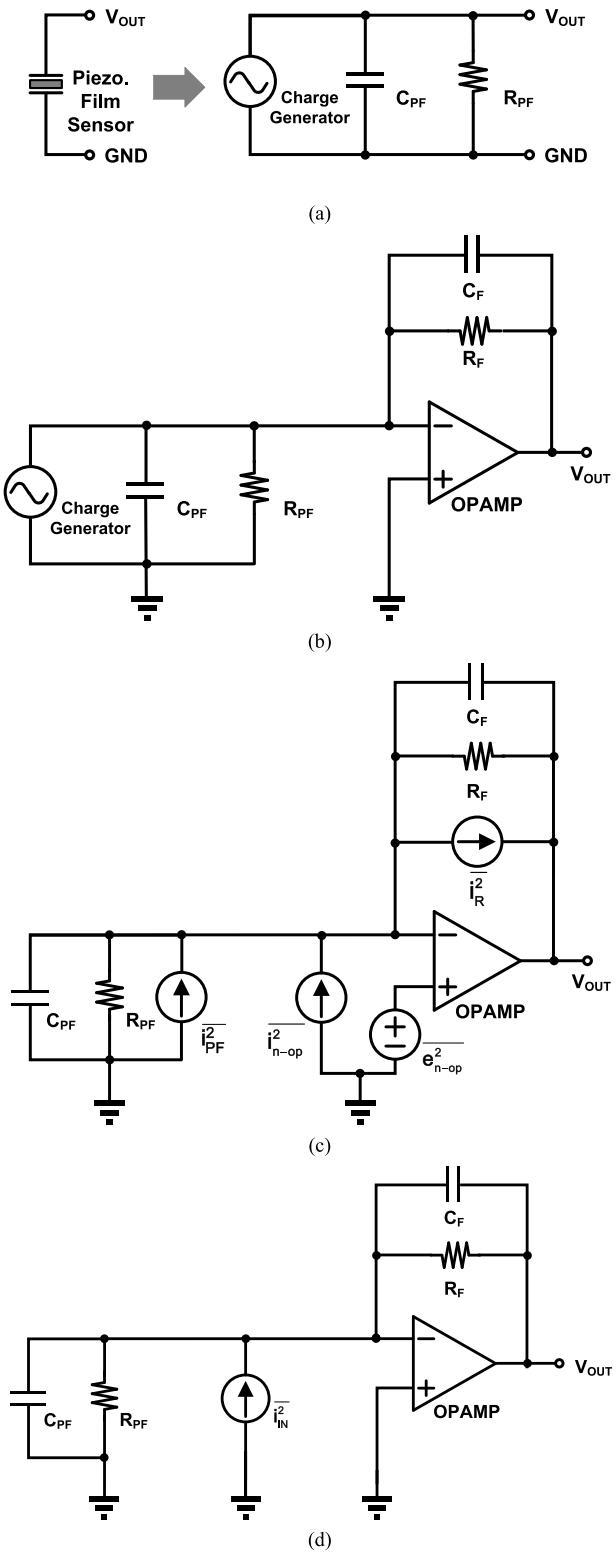

FIGURE 6. (a) Equlvalent circuit of piezoelectric film based force sensor; (b) charge amplifier based readout circuit; (c) noise sources of the circuit and (d) input referred noise source includes all the noise sources.

As the piezoelectric force sensor and readout circuit are uncorrelated noise sources, the input-referred noise power $\overline{i_{IN}^2}$ of the force sensing system is expressed as

$$\overline{i_{IN}^2} = \overline{i_{PF}^2} + \overline{i_{RC}^2}; \tag{7}$$

$\overline{i_{PF}^2}$ and $\overline{i_{RC}^2}$ are the noise power spectrum densities (PSDs) of the piezoelectric touch sensor and the readout circuit, respectively. From Fig. 6 (c), $\overline{i_{RC}^2}$ includes feedback resistor noise $\overline{i_R^2}$ and the input current and voltage noise of the opamp ($\overline{i_{n-op}^2}$ and $\overline{e_{n-op}^2}$, values can be retrieved from operational amplifier product datasheet) [29]. $\overline{i_R^2}$ is expressed as:

$$\overline{i_R^2} = \frac{4kT}{R_F}; \tag{8}$$

where k is the Boltzmann constant and T is the temperature in Kelvin degrees. Note that $\overline{i_{n-op}^2}$ is the shot noise of the input devices. The PSD of the output noise generated by $\overline{e_{n-op}^2}$ is:

$$\begin{aligned}\overline{v_{on}^2} &= \overline{e_{n-op}^2}\left|1+\frac{Z_F}{Z_{PF}}\right|^2 \\ &= \overline{e_{n-op}^2}\frac{(R_{PF}+R_F)^2+4\pi^2 f^2 R_F^2 R_{PF}^2 (C_F+C_{PF})^2}{R_{PF}^2(1+4\pi^2 f^2 R_F^2 R_{PF}^2)};\end{aligned} \tag{9}$$

Here Z_F and Z_{PF} are the feedback and piezoelectric sensor impedance values. As R_{PF} is much higher than R_F, Eq. 9 is simplified as

$$\overline{v_{on}^2} = \overline{e_{n-op}^2}\frac{1+4\pi^2 f^2 R_F^2 (C_F+C_{PF})^2}{(1+4\pi^2 f^2 R_F^2 R_{PF}^2)}; \tag{10}$$

If a CMOS based operational amplifier is utilized, the shot noise can be neglected. Hence, the total input-referred noise PSD is expressed as (Fig. 6 (d))

$$\overline{i_{IN}^2} = \frac{4kT}{R_{PF}} + \frac{4kT}{R_F} + \overline{e_{n-op}^2}\left[\frac{1}{R_F^2} + (2\pi f)2(C_F+C_{PF})^2\right]; \tag{11}$$

If we assume the force strength is linearly increased within a "press" period (assumed to be 0.1s) and that the sampling frequency (f_S) is 100Hz (to ensure that we can accurately interpret the applied force). Then the signal energy (E_{Signal}) is calculated as:

$$E_{Signal} = \frac{Q_T^2}{2C_{PF}f_S}; \tag{12}$$

here Q_T is the total generated charge during the "press" period. Furthermore, if a 1MΩ feedback resistor and a 10nf feedback capacitor are used, the corresponding SNR at location 1 of stack-up 1 is around 59.1dB at room temperature. This indicates that high detection sensitivity is achieved. The force strength could be accurately interpreted.

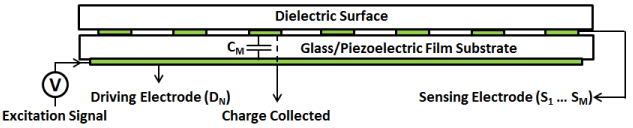

FIGURE 7. Cross view stack-up 1 with glass and piezoelectric material as substrate for electrodes.

B. ELECTROSTATICS ANALYSIS

As the substrate of the touch sensors is changed from glass to piezoelectric film, the mutual capacitance (C_M) in Fig. 7 is decreased with the drop of dielectric coefficient. For force sensing, we need to consider if the applied force will change the distance between the electrodes to further affect the capacitance measurement, as the Young's modulus of the piezoelectric film is much smaller than glass. In the simulation, a 5N force is applied at location 5 of the dielectric surface (panel glass). The capacitance (7.76pC) remains constant before and after the applied force, indicating that the capacitance change is negligible.

VI. CONCLUSION

In this paper, piezoelectric film based TSP are proposed for force sensing in capacitive touch screen panels. With the presented technique, a dynamic force applied on the touch panel can be accurately detected even when the panel's displacement is very small. From the theoretical and numerical results, a good responsivity is achieved at 0.42 V/N and the corresponding SNR is 59.1dB. Hence the presented work provides a revolutionary solution for implementing force sensing in capacitive touch panels.

REFERENCES

[1] G. Walker, *Fundamentals of Projected-Capacitive Touch Technology*. Santa Clara, CA, USA: Intel Corp., Jun. 2014.
[2] L. Zhang, J. Saboune, and A. El Saddik, "Transforming a regular screen into a touch screen using a single Webcam," *IEEE J. Display Technol.*, vol. 10, no. 8, pp. 647–659, Aug. 2014.
[3] B. Detwiler. (Oct. 2015). iPhone 6S teardown reveals upgrades galore, similar hardware layour. CNET Blog. [Online]. Available: http://www.cnet.com/news/iphone-6s-teardown-reveals-upgrades-galore-similar-hardware-layout/
[4] H. Kawai, "The piezoelectricity of Poly (vinylidene Fluoride)," *Jpn. J. Appl. Phys.*, vol. 8, no. 7, p. 975, 1969.
[5] F. Liu, N. A. Hashim, Y. Liu, M. R. M. Abed, and K. Li, "Progress in the production and modification of PVDF membranes," *J. Membrane Sci.*, vol. 375, nos. 1–2, pp. 1–27, Jun. 2011.
[6] C. K. O'Sullivan and G. G. Guilbault, "Commercial quartz crystal microbalances—Theory and applications," *Biosensors Bioelectron.*, vol. 14, nos. 8–9, pp. 663–670, Dec. 1999.
[7] R. Lahtinen, T. Muukkonen, J. Koskinen, S. P. Hannula, and O. Heczko, "A piezopaint-based sensor for monitoring structure dynamics," *Smart Mater. Struct.*, vol. 16, no. 6, pp. 2571–2576, Oct. 2007.
[8] A. Manbachi and R. S. C. Cobbold, "Development and application of piezoelectric materials for ultrasound generation and detection," *Ultrasound*, vol. 19, no. 4, pp. 187–196, Nov. 2011.
[9] A. Nathan and B. Henry, *Microtransducer CAD: Physical and Computational Aspects* (Computational Microelectronics). Vienna, Austria: Springer 1999.
[10] F. Maseeh, M. A. Schmidt, M. G. Allen, and S. D. Senturia, "Calibrated measurements of elastic limit, modulus, and the residual stress of thin films using micromachined suspended structures," in *Proc. IEEE Solid-State Sens. Actuator Workshop*, Jun. 1988, pp. 6–9.

[11] *Specialty Glass Products Technical Reference Document*, Corning Inc., Corning, NY, USA, Aug. 2012.
[12] B. Mohammadi, A. A. Yousefi, and S. M. Bellah, "Effect of tensile strain rate and elongation on crystalline structure and piezoelectric properties of PVDF thin films," *Polymer Test.*, vol. 26, no. 1, pp. 42–50, Feb. 2007.
[13] J. G. Speight, *Norbert Adolph Lange*, 16th ed. New York, NY, USA: McGraw-Hill, 2005.
[14] *The Future is Flexible: Corning Willow Glass, Technique Datasheet*, Corning Inc., Corning, NY, USA, 2012.
[15] S. Lu, Y. Zhang, and W. Dong, "Research on the relationship between the curvature and the sensitivity of curved PVDF sensor," *Proc. SPIE*, vol. 9446, p. 94461Y, Feb. 2015.
[16] P. Saketi *et al.*, "PVDF microforce sensor for the measurement of Z-directional strength in paper fiber bonds," *Sens. Actuators A, Phys.*, vol. 222, pp. 194–203, Feb. 2015.
[17] T. Sharma, K. Aroom, S. Naik, B. Gill, and J. X. J. Zhang, "Flexible thin-film PVDF-TrFE based pressure sensor for smart catheter applications," *Ann. Biomed. Eng.*, vol. 41, no. 4, pp. 744–751, Dec. 2012.
[18] Y. Yu, X. Zhao, Y. Wang, and J. Qu, "A study on PVDF sensor using wireless experimental system for bridge structure local monitoring," *Telecommun. Syst.*, vol. 52, no. 4, pp. 2357–2366, 2013.
[19] Y. F. Jia, Q. S. Ni, X. J. Chen, C. Ju, K. L. Xing, and T. H. Jin, "Simulation and experiment of PVDF temperature sensor," *Appl. Mech. Mater.*, vols. 303–306, pp. 109–113, Feb. 2013.
[20] P. C. A. Hammes and P. P. L. Regtien, "An integrated infrared sensor using the pyroelectric polymer PVDF," *Sens. Actuators A, Phys.*, vol. 32, nos. 1–3, pp. 396–402, Apr. 1992.
[21] B. Ren and C. J. Lissenden, "PVDF Multielement lamb wave sensor for structural health monitoring," *IEEE Trans. Ultrason., Ferroelectr., Freq. Control*, vol. 63, no. 1, pp. 178–185, Jan. 2016.
[22] D.-H. Kim, B. Kim, and H. Kang, "Development of a piezoelectric polymer-based sensorized microgripper for microassembly and micromanipulation," *Microsyst. Technol.*, vol. 10, no. 4, pp. 275–280, May 2004.
[23] Y. Gu, R. L. Clark, C. R. Fuller, and A. C. Zander, "Experiments on active control of plate vibration using piezoelectric actuators and polyvinylidene fluoride (PVDF) modal sensors," *J. Vibrat. Acoust.*, vol. 116, no. 3, pp. 303–308, Jul. 1994.
[24] F. Charette, A. Berry, and C. Guigou, "Active control of sound radiation from a plate using a polyvinylidene fluoride volume displacement sensor," *J. Acoust. Soc. Amer.*, vol. 103, no. 3, p. 1493, 1998.
[25] L. Ma, S. N. Melkote, J. B. Morehouse, J. B. Castle, J. W. Fonta, and M. A. Johnson, "Thin-film PVDF sensor-based monitoring of cutting forces in peripheral end milling," *J. Dyn. Syst. Meas. Control*, vol. 134, no. 5, p. 051014, Jul. 2012.
[26] L. Maiolo *et al.*, "A comparison among low temperature piezoelectric flexible sensors based on polysilicon TFTs for advanced tactile sensing on plastic," *IEEE J. Display Technol.*, vol. 12, no. 3, pp. 209–213, Mar. 2016, doi: 10.1109/JDT.2015.2439737.
[27] P. G. Lemarie-Rieusset, *Recent Developments in the Navier–Stokes Problem*. Boca Raton, FL, USA: CRC Press, 2002.
[28] *Interfacing Piezo Film to Electronics*, Measurement Specialties, Inc., Schaffhausen, Switzerland, Mar. 2006.
[29] M. Crescentini, M. Bennati, M. Carminati, and M. Tartagni, "Noise limits of CMOS current interfaces for biosensors: A review," *IEEE Trans. Biomed. Circuits Syst.*, vol. 8, no. 2, pp. 278–292, Apr. 2012.

SHUO GAO received the M.Sc. degree in electrical engineering from the University of Ottawa, Canada, in 2013. He is currently pursuing the Ph.D. degree with the Hetero-Genesys Laboratory, University of Cambridge. He is a recipient of China Scholarship Council Scholarship for the Ph.D. program. He was an Optical Fiber System Engineer with Ciena Corporation, Ottawa, Canada. He is also a Technical Adviser of Cambridge Touch Technologies Ltd., Cambridge, U.K. His research interests include touch interactivity and RF system for flexible electronics.

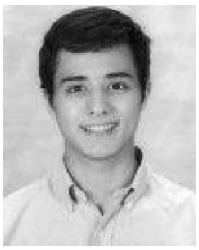

VICTOR ARCOS is currently pursuing the M.Eng. degree with the University of Cambridge, and a member of Trinity College. He is currently with the Hetero-Genesys Laboratory, where he is currently involved in touch screen panel project. Previously, he did internship as an Engineer with Marshall Aerospace Cambridge. His research interests include touch screen panels and flexible electronics.

AROKIA NATHAN (S'84–M'87–SM'99–F'10) received the Ph.D. degree in electrical engineering from the University of Alberta. He held a postdoctoral position with LSI Logic Corp., USA, and ETH Zurich, Switzerland. He joined the University of Waterloo, Canada, where he held the DALSA/NSERC Industrial Research Chair in sensor technology and subsequently the Canada Research Chair in nano-scale flexible circuits. He was a recipient of the 2001 NSERC E.W.R. Steacie Fellowship. In 2006, he moved to the U.K. to take up the Sumitomo Chair of Nanotechnology with the London Centre for Nanotechnology, University College London, where he received the Royal Society Wolfson Research Merit Award. He has held visiting professor appointments with the Physical Electronics Laboratory, ETH Zürich, and the Engineering Department, Cambridge University, U.K. He holds the Chair of Photonic Systems and Displays with the Department of Engineering, Cambridge University. He has authored over 500 papers in the field of sensor technology, CAD, thin film transistor electronics, and is a co-author of four books. He has over 50 patents filed/awarded and has founded/co-founded four spin-off companies. He serves on technical committees and editorial boards in various capacities. He is currently a Chartered Engineer, U.K., a fellow of the Institution of Engineering and Technology, U.K., and the IEEE/EDS Distinguished Lecture.